

Simultaneous measurement of in-plane and out-of-plane displacements using pseudo-Wigner-Hough transform

Rishikesh Kulkarni and Pramod Rastogi*

*Applied Computing and Mechanics Laboratory, Ecole polytechnique fédérale de Lausanne,
1015 Lausanne, Switzerland*

[*pramod.rastogi@epfl.ch](mailto:pramod.rastogi@epfl.ch)

Abstract: A new method based on pseudo-Wigner-Hough transform is proposed for the simultaneous measurement of the in-plane and out-of-plane displacements using digital holographic moiré. Multiple interference phases corresponding to the in-plane and out-of-plane displacement components are retrieved from a single moiré fringe pattern. The segmentation of the interference field allows us to approximate it with a multicomponent linear frequency modulated signal. The proposed method accurately and simultaneously estimates all the phase parameters of the signal components without the use of any signal separation techniques. Simulation and experimental results demonstrate the efficacy of the proposed method and its robustness against the variations in object beam intensity.

© 2014 Optical Society of America

OCIS codes: (120.2880) Holographic interferometry; (120.2650) Fringe analysis; (120.4290) Nondestructive testing.

References and links

1. P. Picart, D. Mounier, and J. M. Desse, "High-resolution digital two-color holographic metrology," *Opt. Lett.* **33**, 276–278 (2008).
2. P. Picart, E. Moisson, and D. Mounier, "Twin-sensitivity measurement by spatial multiplexing of digitally recorded holograms," *Appl. Opt.* **42**, 1947–1957 (2003).
3. C. Kohler, M. R. Viotti, and A. G. Albertazzi Jr., "Measurement of three-dimensional deformations using digital holography with radial sensitivity" *Appl. Opt.* **49**, 4004–4009 (2010).
4. S. Okazawa, M. Fujigaki, Y. Morimoto, and T. Matui, "Simultaneous measurement of out-of-plane and in-plane displacements by phase-shifting digital holographic interferometry," *Appl. Mech. Mater.* **3-4**, 223–228 (2005).
5. G. Rajshekhar, S. S. Gorthi, and P. Rastogi, "Simultaneous multidimensional deformation measurements using digital holographic moiré," *Appl. Opt.* **50**, 4189–4197 (2011).
6. G. Rajshekhar, S. S. Gorthi, and P. Rastogi, "Estimation of multiple phases from a single fringe pattern in digital holographic interferometry," *Opt. Express* **20**, 1281–1291 (2012).
7. R. Kulkarni and P. Rastogi, "Multiple phase estimation in digital holographic interferometry using product cubic phase function," *Opt. Laser Eng.* **51**, 1168–1172 (2013).
8. K. Pokorski and K. Patorski, "Separation of complex fringe patterns using two-dimensional continuous wavelet transform," *Appl. Opt.* **51**, 8433–8439 (2012).
9. S. Barbarossa, "Analysis of multicomponent lfm signals by a combined wigner-hough transform," *IEEE T. Signal Process.* **43**, 1511–1515 (1995).
10. L. Cirillo, A. Zoubir, and M. Amin, "Parameter estimation for locally linear fm signals using a time-frequency hough transform," *IEEE T. Signal Process.* **56**, 4162–4175 (2008).
11. D. S. Pham and A. M. Zoubir, "Analysis of multicomponent polynomial phase signals," *IEEE T. Signal Process.* **55**, 56–65 (2007).
12. S. S. Gorthi, G. Rajshekhar, and P. Rastogi, "Strain estimation in digital holographic interferometry using piecewise polynomial phase approximation based method," *Opt. Express* **18**, 560–565 (2010).
13. G. Rajshekhar and P. Rastogi, "Fringe analysis: Premise and perspectives," *Opt. Laser Eng.* **50**, iii–x (2012).

1. Introduction

Digital holographic interferometry (DHI) is a prominent measurement technique for deformation analysis and non-destructive testing applications because of its non-invasive and whole-field measurement capability. The information on object deformation can be reliably obtained by accurately estimating the interference phase of a recorded fringe pattern. However, this method is in general effective for the measurement of a single component of displacement.

Advanced techniques employing multiple object beams have been proposed for multidimensional deformation measurement. The multiple interference phases associated with the object beams can be algebraically manipulated to obtain the components of object displacement. Different techniques have been proposed for the estimation of these interference phases. The basic precept behind the techniques proposed in [1, 2, 3] is to obtain incoherently mixed holograms generated by multiple reference and object beam-pairs. In [4], phase shifting technique is employed to separately record the holograms for each object beam. On the other hand, the techniques proposed in [5, 6, 7] employ two object beams paired to the same reference beam resulting in an easy to handle optical set-up. The recording of wavefronts in this manner gives rise to the formation of a holographic moiré pattern. Subsequently, signal processing approaches have been applied to extract multiple phase information from the so formed moiré fringes. Recently, another approach based on two dimensional continuous wavelet transform has been proposed in [8] to separate the fringe components from a single moiré fringe pattern. This method provides the wrapped form of the separated interference phases which further necessitates the use of unwrapping algorithms.

The multiple phase estimation method proposed in [5] requires a careful adjustment of the carrier frequency in order to separate the signal components in spectral domain which is practically difficult. Moreover, the estimated phases are in wrapped form which necessitate the use of complex unwrapping algorithms to obtain the unwrapped phase maps. Although these limitations are avoided in the phase estimation methods proposed in [6, 7], the inherent sequential phase parameter estimation procedure involved in them severely limits their ability to accurately estimate the multiple phases. Furthermore, the accuracy of phase estimation depends upon object beam intensity settings used to establish amplitude discrimination.

In the present work, a new method based on pseudo-Wigner-Hough transform is proposed for the multiple interference phase estimation from a single moiré fringe pattern. The segmentation of the moiré interference field allows us to represent it as a multicomponent linear frequency modulated signal. The proposed method benefits from the amalgamation of the signal processing and image processing tools to simultaneously provide the accurate estimation of phase parameters of all the signal components without the use of carrier frequency. These phase parameters are further utilized for the estimation of the interference phases. The theory of the proposed method is explained in Section 2. The simulation and experimental results are provided in Section 3 followed by conclusion.

2. Theory

Consider that the object is illuminated with two object beams placed symmetrically to the normal to the object surface. Two holograms are recorded, each one before and after the deformation of the object. The numerical reconstruction of holograms is performed using digital Fresnel transform to obtain the complex amplitudes of the optical wavefields for each object state. The conjugate multiplication of the complex amplitudes generates an interference field with two components. The phases of these two components carry the information on object deformation. The interference field can be represented as,

$$\Gamma(x, y) = A_1(x, y) \exp[j\Delta\phi_1(x, y)] + A_2(x, y) \exp[j\Delta\phi_2(x, y)] + \eta(x, y) \quad (1)$$

The interference field $\Gamma(x,y)$ is of the size $N \times N$ pixels. The pixels along the columns and rows are represented by x and y , respectively. $A_1(x,y)$ and $A_2(x,y)$ are the slowly varying or constant amplitudes; $\Delta\phi_1(x,y)$ and $\Delta\phi_2(x,y)$ represent the interference phases and $\eta(x,y)$ is the complex additive white Gaussian noise. In general, the interference phases are continuous functions of spatial coordinates x and y . Consequently, they can be approximated with the polynomials of appropriate order. However, if the interference phases vary rapidly, the required order for polynomial approximation of phases could be correspondingly high. The accuracy of phase parameter estimation decreases with the increase in the polynomial order especially in the case of multicomponent signals. Therefore, lower order polynomial approximation of interference phases is achieved by dividing the interference field into a number of non-overlapping segments L in each column x or in each row y . Although, further analysis is carried out considering the signal segmentation in each column x , it should be noted that the same analysis is true in case of signal segmentation in each row y also. Over these segments, the interference phases are approximated with second order polynomial functions of y with a multicomponent linear frequency-modulated signal representation of the interference field. Thus, for a given column x , the interference field in the segment l with $l \in (1,L)$ can be represented as,

$$\Gamma_l(y) = A_{l1}(y) \exp[j\Delta\phi_{l1}(y)] + A_{l2}(y) \exp[j\Delta\phi_{l2}(y)] + \eta_l(y) \quad (2)$$

where,

$$\Delta\phi_{l1}(y) = a_{l1} + b_{l1}y + c_{l1}y^2 \quad (3)$$

$$\Delta\phi_{l2}(y) = a_{l2} + b_{l2}y + c_{l2}y^2 \quad (4)$$

The phase parameters $a \in \{a_{l1}, a_{l2}\}$, $b \in \{b_{l1}, b_{l2}\}$, $c \in \{c_{l1}, c_{l2}\}$ correspond to *initial phase*, *mean spatial frequency* and *sweep rate*, respectively. From the above equations, it can be understood that the phase parameters a , b and c have to be accurately estimated for reliable estimation of the interference phases.

A combined form of Wigner-Ville-Distribution (WVD) and Hough transform, termed as Wigner-Hough-transform (WHT), has been proposed [9] for analyzing linear frequency-modulated signals. The WVD of a linear frequency-modulated signal produces a distribution of energy concentrated along a straight line in space-frequency (s-f) plane. Thus, the problem of analyzing linear frequency-modulated signal can be looked upon more as the detection of a linear pattern in the s-f plane. The Hough-transform, a popular technique used in the image processing for the detection of lines in images, is applied for the detection of a linear pattern in the s-f plane. The Hough transform of the WVD of a given signal essentially transforms it from the s-f domain to the phase parameter domain. The peak observed in the phase parameter domain provides the estimates of the signal phase parameters. These estimates are subsequently utilized as initial values of the optimization algorithm to obtain accurate values of phase parameters.

The WHT method proves to be equally effective in the case of multicomponent signal analysis. The WVD of a multicomponent signal produces a distribution of energy in the s-f plane corresponding to the multiple signal components along with the unwanted cross terms. The cross terms arise on account of the bilinear property of the WVD. This property of WVD seriously hampers its ability to analyze the multicomponent signal. It is observed that the energy distribution corresponding to the multiple signal components is positive whereas the energy distribution of cross terms oscillates between positive and negative values. This attribute is exploited by WHT. In the WHT of given multicomponent signal, the effect of cross terms produced by WVD is removed by the Hough transform due to the inherent integration process involved in it. Thus, the WHT can accurately estimate the phase parameters of all the signal components simultaneously.

However, the advantages of WHT come at the price of high computational cost. This led to the development of the combined use of pseudo-Wigner-Ville-Distribution (PWVD) and Hough

transform, more appropriately termed as pseudo-Wigner-Hough-transform (PWHT) [10]. The PWHT of the interference field $\Gamma_l(y)$ can be represented as,

$$PWHT(\theta) = \sum_{y=M}^{N_L-M-1} \sum_{l=-M}^M \Gamma_l(y+l) \Gamma_l^*(y-l) \exp(j2\omega(y; \theta)) \quad (5)$$

where, $N_L = N/L$ is the length of $\Gamma_l(y)$; M is the parameter defining window length, $W = 2M + 1$; θ represents the domain of phase parameters b and c ; $\omega = b + cy$. The optimum value of $M = 0.1N_L$ has been suggested [10] for optimal estimation of phase parameters. The number of peaks observed in the PWHT of a given multicomponent signal indicates the number of signal components present in it. The locations of these peaks provide the estimates of phase parameters b and c of all the signal components. PWHT is computationally more efficient as compared to WHT due to the windowing involved in PWVD. Additionally, the width of peak observed in PWHT parameter space is much larger than that observed for the WHT. This suggests that the PWHT offers improved numerical properties during optimization than that offered by the WHT. It is required to ensure that the initial estimates of phase parameters calculated using PWHT are accurate enough so that the optimization algorithm converges to true phase parameter values. In order to achieve this, peak detection in PWHT is performed on the grid of phase parameters b and c with appropriate grid spacings of Δ_b and Δ_c , respectively. The values of Δ_b and Δ_c can be calculated as [10],

$$\Delta_b = \frac{\pi}{1.4W} \quad (6)$$

$$\Delta_c = \frac{\pi}{(-1.19M^2 + 1.2MN_L - 3M + 0.4N_L + 17.5)} \quad (7)$$

In the proposed method, the interference phases are estimated in a given column x one at a time. It is therefore required to group the estimated phases together with their respective counterparts from the other columns to obtain the complete 2D phase maps. To achieve this, a simple amplitude discrimination criteria is proposed. Different intensity levels are set up for each of the two object beams which result in different amplitudes of signal components in Eq.(1). It should be noted that the amplitude discrimination criteria is not used for the estimation of the phase parameters but only to discriminate between the estimated phases. On the contrary, the phase parameters of all signal components are estimated simultaneously. Consequently, the inherent error propagation effect of the sequential phase parameter estimation procedure based on amplitude discrimination criteria proposed in [7] is avoided in the PWHT based phase estimation method. Furthermore, the ratio of the amplitudes of the individual components need not be controlled precisely because its variation does not affect the phase parameter estimation accuracy. The procedure of multicomponent signal analysis using PWHT is explained in the following steps:

1. Set up the amplitude discrimination criteria with $A_1 > A_2$.
2. Obtain the estimates of $\{b_{l1}, b_{l2}\}$ and $\{c_{l1}, c_{l2}\}$ by calculating PWHT of $\Gamma_l(y)$ using Eq. (5) - Eq.(7).
3. Calculate the estimates of $\{a_{l1}, a_{l2}\}$ and $\{A_{l1}, A_{l2}\}$ using following equations:

$$\hat{a}_{lk} = \text{angle} \left\{ \frac{1}{N_L} \sum_{y=-\frac{N_L-1}{2}}^{\frac{N_L-1}{2}} \Gamma_l(y) \exp[-j(\hat{b}_{lk}y + \hat{c}_{lk}y^2)] \right\} \quad (8)$$

$$\hat{A}_{lk} = \left| \frac{1}{N_L} \sum_{y=-\frac{N_L-1}{2}}^{\frac{N_L-1}{2}} \Gamma_l(y) \exp[-j(\hat{b}_{lk}y + \hat{c}_{lk}y^2)] \right| \quad (9)$$

where, $k \in \{1, 2\}$.

Although the error propagation effect is eliminated by PWHT, there exists an inherent bias caused by the multiple peaks observed in parameter space in case of a multicomponent signal. These peaks disturb one another due to the peaks' spreading. As a result, the peaks' locations get shifted from the true phase parameter values. To avoid this problem, bias reduction operation is performed in which the contribution of the lower amplitude signal component is removed from $\Gamma_l(y)$. Subsequently, the above explained steps (ii) and (iii) are used to re-estimate the phase parameters. These estimates are used as initial values for Nelder-Mead simplex optimization algorithm [11] for further refinement of phase parameters. This operation is repeated for the phase parameter estimation of lower amplitude signal component. With the refined phase parameter estimates, the unwrapped interference phases are estimated using Eq. (3) and Eq. (4) for all the segments in all the columns. The complete 2D phase maps are generated using the phase stitching operation.

3. Simulation and experimental results

Simulations were performed to examine the efficacy of the proposed method. The interference field of size 257×257 was simulated with signal-to-noise ratio (SNR) of 30 dB using two interference phases $\Delta\phi_1(x, y)$ and $\Delta\phi_2(x, y)$ shown in Fig. 1(a) and Fig. 1(b). The ratio of signal amplitudes was set to 1.5 : 1. The moiré fringe pattern i.e. the real part of the interference field, $\Gamma(x, y)$ given in Eq. (1), can be represented as,

$$\Gamma_r(x, y) = A_1(x, y) \cos[\Delta\phi_1(x, y)] + A_2(x, y) \cos[\Delta\phi_2(x, y)] + \eta_r(x, y) \quad (10)$$

where, $\eta_r(x, y)$ is the real part of $\eta(x, y)$. The moiré fringe pattern and Fourier spectrum of the interference field are shown in Fig. 1(c) and Fig. 1(d), respectively. It can be observed that the spectrum of the signal components overlap each other. The proposed technique does not require any addition of carrier frequency for separation of signal components as proposed in [5]. The interference field was divided into $L = 4$ segments in each column. The grid spacings of the parameter space for b and c were calculated using Eq. (6) and Eq. (7). Using these grid spacings, the phase parameters were estimated over a small grid of size 19×12 .

The cosine fringes corresponding to the estimated $\Delta\phi_1(x, y)$ and $\Delta\phi_2(x, y)$ are plotted in Fig. 2(a) and Fig. 2(b), respectively. The error in the estimation of $\Delta\phi_1(x, y)$ and $\Delta\phi_2(x, y)$ are plotted in Fig. 2(c) and Fig. 2(d), respectively. The root-mean-square error (RMSE) in estimation of $\Delta\phi_1(x, y)$ and $\Delta\phi_2(x, y)$ were found to be 0.0558 and 0.0818 radians, respectively. The error in the phase estimation near the segment boundaries can be further reduced using overlapping segments [12, 13], which improves the estimation accuracy, though at a higher computational cost.

The analysis was also performed with the phase estimation method proposed in [7]. In this case, it was found that the phase estimation method failed to accurately estimate the interference phases. The RMSE in estimation of $\Delta\phi_1(x, y)$ and $\Delta\phi_2(x, y)$ were found to be 4.6797 and 13.0087 radians, respectively. This shows that the performance of PWHT based phase estimation is far superior as compared to that proposed in [7]. The simulation study performed in [10] has shown that the PWHT based phase parameter estimation has better performance compared to product high order ambiguity function (PHAF). This indicates that the phase estimation method proposed in this study performs better compared to the method based on PHAF proposed in [6].

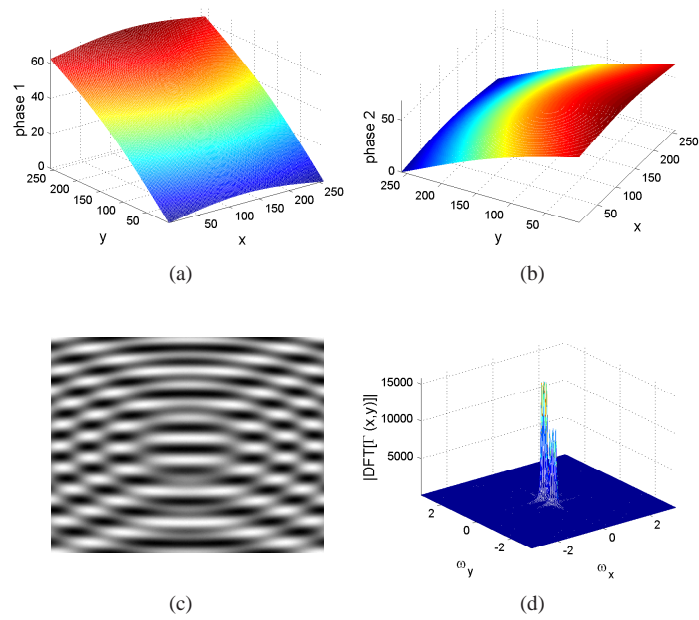


Fig. 1: (a) $\Delta\phi_1(x,y)$ (b) $\Delta\phi_2(x,y)$ (c) moiré fringe pattern (d) Fourier spectrum of interference field. The phase values are in radians.

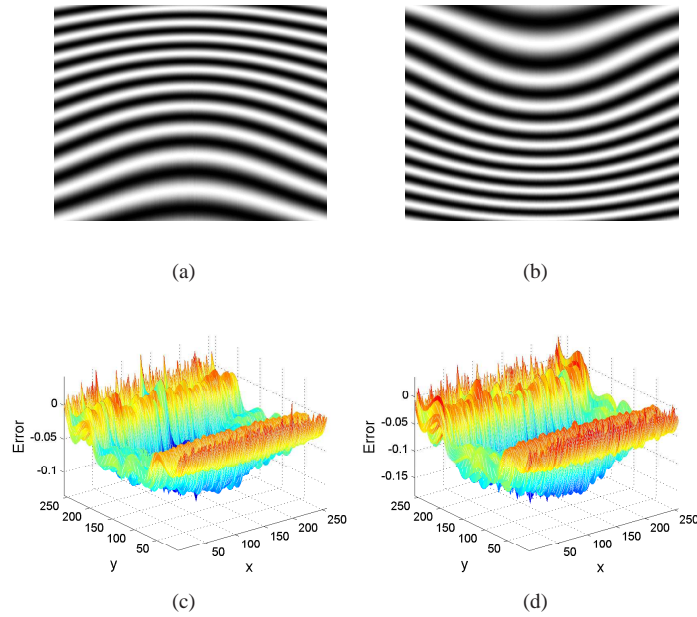


Fig. 2: cosine fringes corresponding to the estimated (a) $\Delta\phi_1(x,y)$ (b) $\Delta\phi_2(x,y)$. Error in estimation of (a) $\Delta\phi_1(x,y)$ (b) $\Delta\phi_2(x,y)$. All values are in radians.

The effect of variations in amplitude ratio on the phase estimation accuracy was also studied. The interference field was simulated with a SNR of 30 dB at different amplitude ratios ($A_1 : A_2$) using the simulated phases shown in Fig. 1(a) and Fig. 1(b). For each case, the calculated RMSE in the estimation of interference phases are given in Table 1. The RMSE values, found to be well below 0.1 radians, indicate that the accuracy of phase estimation is least affected by the variations in amplitude ratio. It should be noted that the variation in estimation error with varying amplitude ratio is mainly caused by the variation in the white Gaussian noise component added in the signal during each simulation run.

Table 1: Phase estimation error in radians at different amplitude ratio

Interference phase	Amplitude ratio ($A_1 : A_2$)				
	1.3	1.5	1.7	1.9	2.1
$\Delta\phi_1(x,y)$	0.0488	0.0558	0.0524	0.0507	0.0520
$\Delta\phi_2(x,y)$	0.0537	0.0818	0.0635	0.0436	0.0499

An important point to note here is that the various phase unwrapping algorithms proposed in the literature are applicable for single interference phase unwrapping only. They are not useful in the case of moiré fringes as it contains multiple interference phases. The proposed method not only extracts the multiple interference phases from a single moiré fringe pattern, but also directly provides the unwrapped phase estimates.

The ability of simultaneous estimation of phase parameters of the signal components of the interference field allows the proposed technique to outperform the previously reported phase estimation methods in [6, 7].

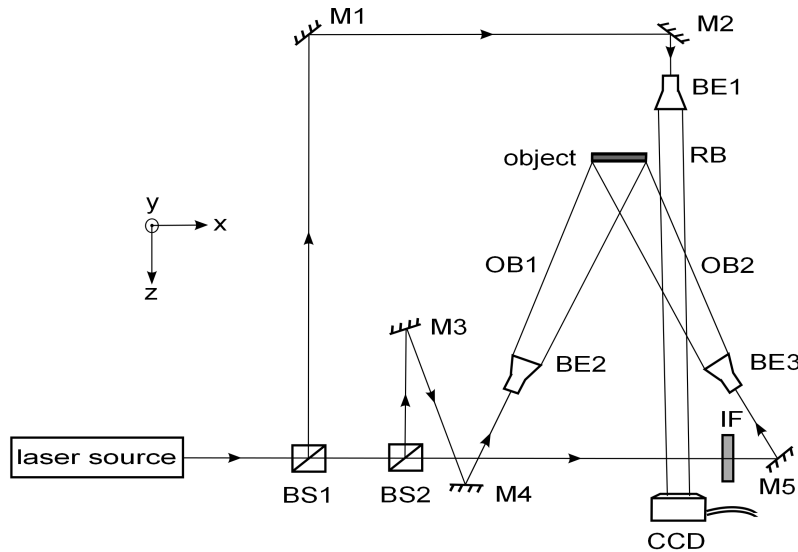


Fig. 3: Experimental set up: BS1-BS2, beam splitters; BE1-BE3, beam expanders; M1-M5, mirrors; OB1-OB2, object beams; RB, reference beam; IF, beam intensity filter.

The experimental set-up consisted of two object beams OB1 and OB2 and a reference beam (RB) derived from a Coherent Verdi (Coherent, Inc., USA) laser source of wavelength 532 nm as shown in Fig. 3. Two distinct intensities were set for the two object beams using a beam intensity filter (IF) in the object beam OB2 arm to establish the amplitude discrimination criteria. The variable filter provides the flexibility of setting different object beam intensity ratios. Holograms were recorded with a CCD camera (XCL-U1000, Sony Corporation, Japan) of size 1600×1200 pixels. A circular membrane with clamped edges was used as a light diffusing object. The object was subjected to out-of-plane deformation with a point load and an in-plane rigid body rotation was superimposed on this deformation. The coordinate system used is also shown in the figure.

The recorded moiré fringe pattern is shown in Fig. 4(a). The Fourier spectrum of the interference field is shown in Fig. 4(b). The proposed method was applied for the interference phase estimation. The estimated interference phases are shown in Fig. 4(c) and Fig. 4(d). Due to the symmetrical illumination of the object, the sum and difference of the interference phases provide the out-of-plane and in-plane components of displacement, respectively [5]. The sum and differences of the estimated phases are shown in Fig. 5(a) - Fig. 5(d) along with their wrapped forms.

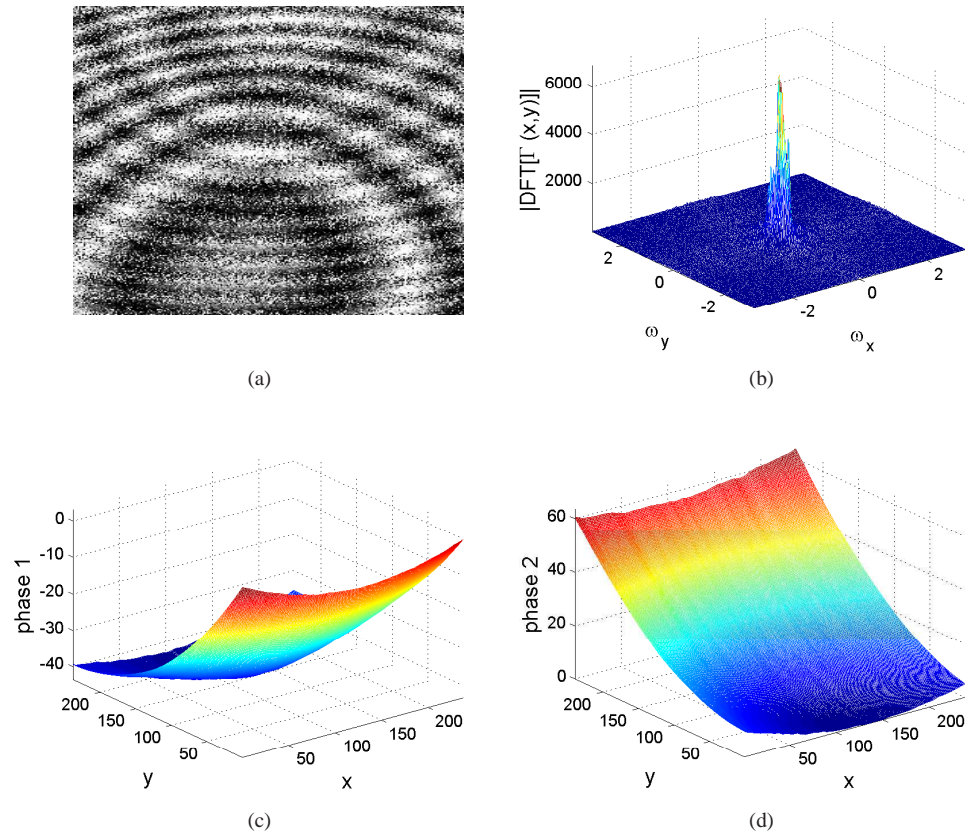


Fig. 4: (a) Moiré fringe pattern (b) Fourier spectrum of interference field (c) Estimated $\Delta\phi_1(x,y)$ (d) Estimated $\Delta\phi_2(x,y)$. The phase values are in radians.

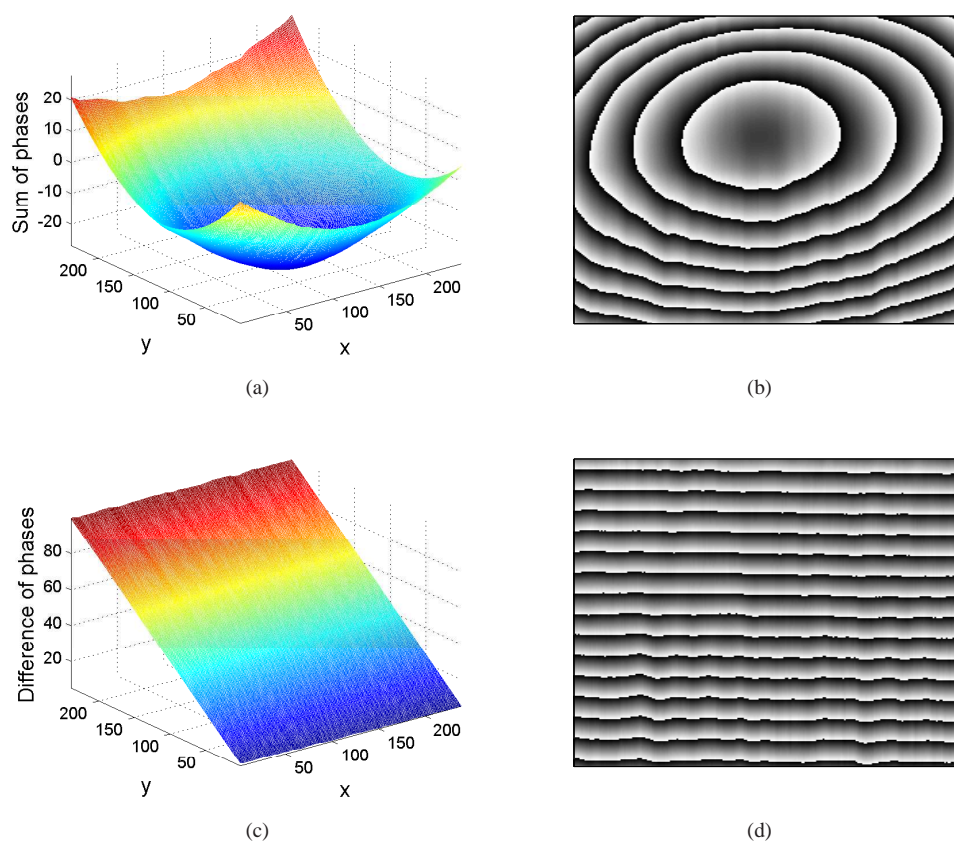


Fig. 5: (a) Sum of phases (b) wrapped form of sum of phases (c) Difference of phases (d) wrapped form of difference of phases. The phase values are in radians.

4. Conclusion

This paper proposes a new method for simultaneous measurement of in-plane and out-of-plane displacement based on pseudo-Wigner-Hough transform using a single moiré fringe pattern. The PWHT based phase parameter estimation is successfully implemented for the accurate estimation of multiple interference phases. The proposed phase estimation method is robust against the object beam intensity variations, making the method suitable for practical applications. Both simulation and experimental results are provided to substantiate the effectiveness of the proposed method in case of two dimensional displacement measurement.